3-12-2019

Kinetics of liquid-assisted densification during flash sintering of ceramic nanoparticles

Rachman Chaim

Kinetics of Liquid-film Assisted Densification during Flash Sintering of Ceramic Nanoparticles

Rachman Chaim

Department of Materials Science and Engineering,

Technion – Israel Institute of Technology

Haifa 32000 Israel

Acknowledgments

- *Prof. Claude Estournes*   *CIRIMAT, Toulouse, France*
- *Prof. Nahum Frage*   *Ben-Gurion University, Israel*
- *Prof. Arturo Dominguez-Rodriguez, Sevilla Univ., Spain*
- *Dr. Sergei Kalabukhov*   *Ben-Gurion University, Israel*
- *Geoffroy Chevallier*   *CIRIMAT, Toulouse, France*

Outline

- *Densification mechanisms during the Flash Sintering*

- *Formation of a liquid-film*

    - *Thermodynamics and Kinetics*

    - *Densification via liquid-film capillary forces*

    - *The lack of residual amorphous layer*

- *Summary & Conclusions*

Densification mechanisms *suggested* for Flash Sintering

Solid-state sintering ⟺ Liquid-film assisted sintering

Avalanche of point defects ⟺ *Liquid film*

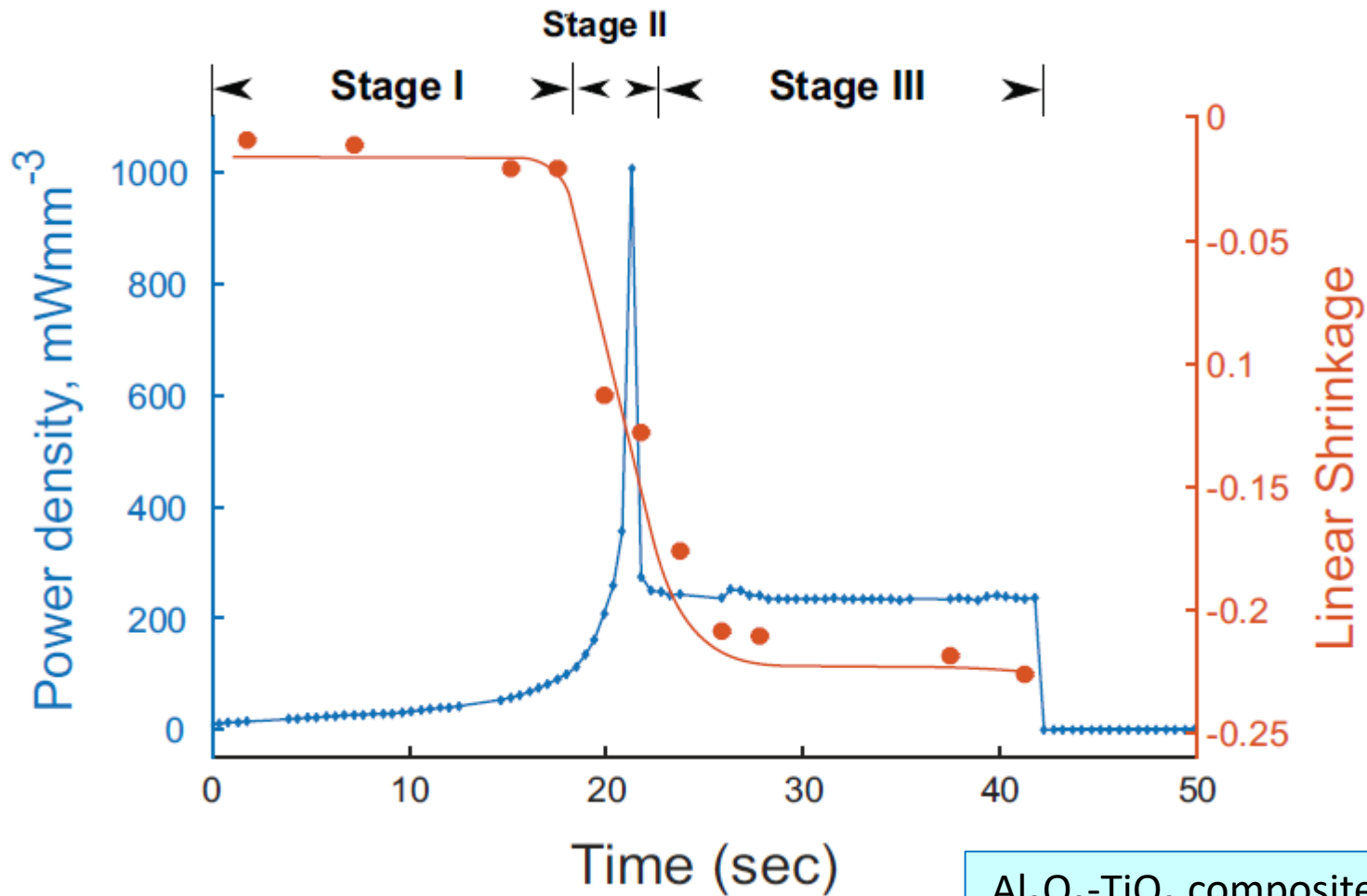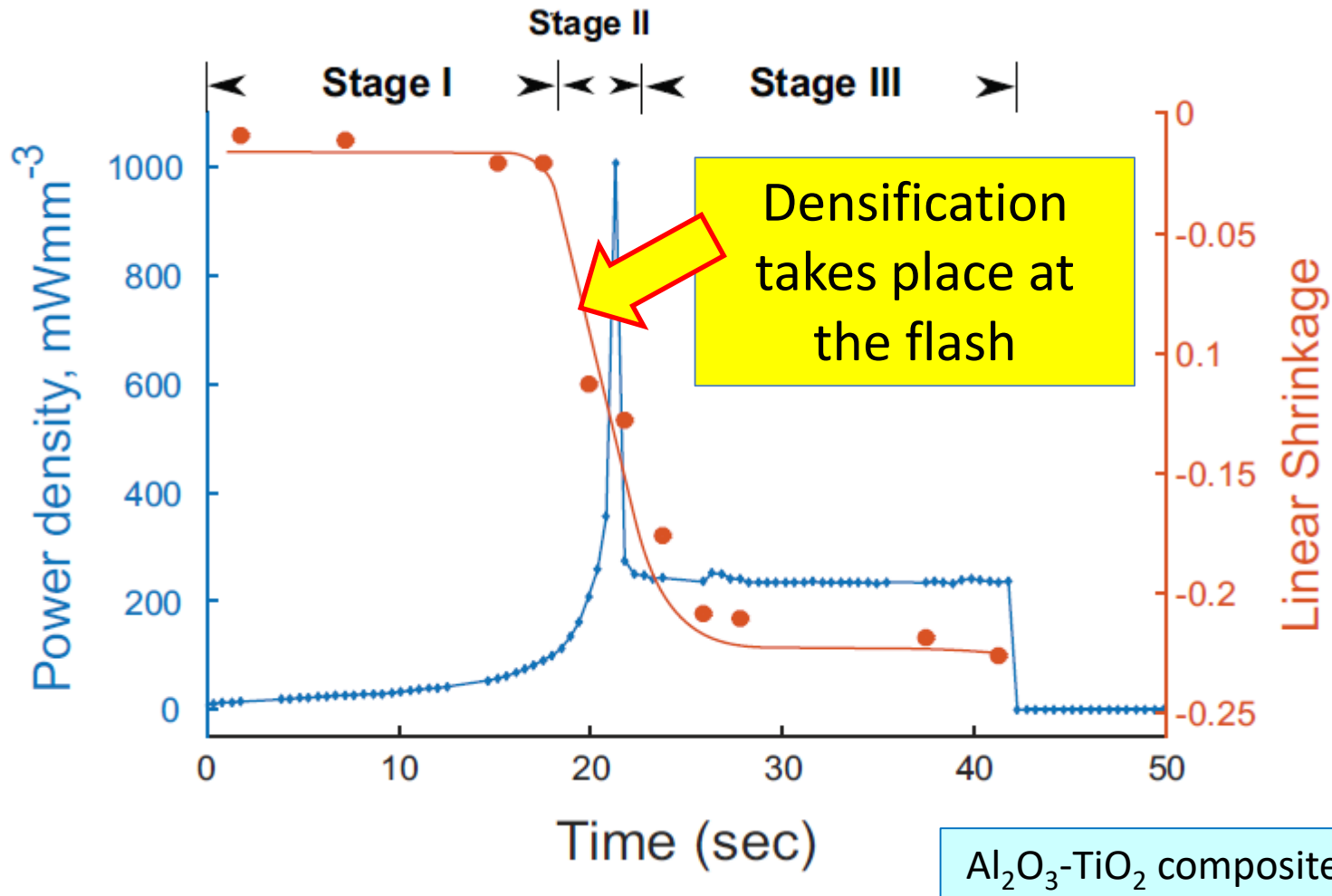Bulk phenomenon ⟺ Surficial / Interfacial phenomenon

The power peak is Artificial

Al$_2$O$_3$-TiO$_2$ composite

*Jha, Lebrun, Raj, J. Eur. Ceram. Soc. **36** (2016) 733*

The power peak is Artificial

Stage II

Stage I | Stage III

Power density, mWmm^{-3} vs Linear Shrinkage

Densification takes place at the flash

Al$_2$O$_3$-TiO$_2$ composite

*Jha, Lebrun, Raj, J. Eur. Ceram. Soc. **36** (2016) 733*

7

The power peak is *Artificial*

Energy input for densification mechanism

Al$_2$O$_3$-TiO$_2$ composite

*Jha, Lebrun, Raj, J. Eur. Ceram. Soc. **36** (2016) 733*
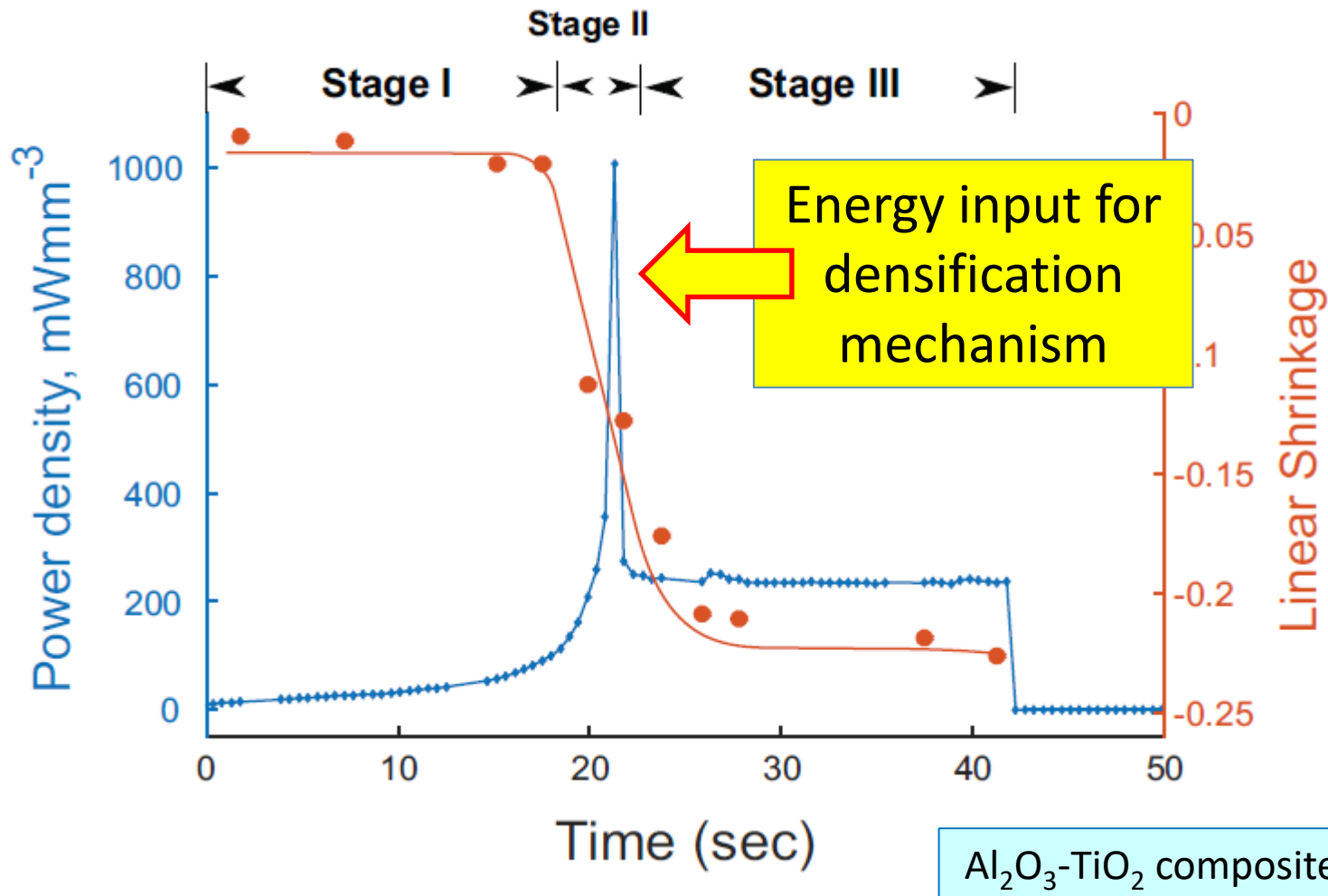
Flash sintering of dielectric nanoparticles as a percolation phenomenon through a softened film

Rachman Chaim,[1,a)] Geoffroy Chevallier,[2,b)] Alicia Weibel,[2,c)] and Claude Estournès[2,d)]

[1]*Department of Materials Science and Engineering, Technion - Israel Institute of Technology, Haifa 32000, Israel*

[2]*Université de Toulouse, CIRIMAT, CNRS INPT UPS, Université Paul-Sabatier, 118 route de Narbonne, F-31062 Toulouse cedex 9, France*

Recent work [Biesuz *et al.*, J. Appl. Phys. **120**, 145107 (2016)] showed analogies between the flash sintering and dielectric breakdown in α-aluminas pre-sintered to different densities. Here, we show that flash sintering of dielectric nanoparticles can be described as a universal behavior by the percolation model. The electrical system is composed of particles and their contact point resistances, the latter softened first due to preferred local Joule heating and thermal runaway during the flash. Local softening has a hierarchical and invasive nature and propagates between the electrodes. The flash event signals the percolation threshold by invasive nature of the softened layer at the particle surfaces. Rapid densification is associated with local particle rearrangements due to attractive capillary forces induced by the softened film at the particle contacts. Flash sintering is a critical phenomenon with a self-organizing character. The experimental electric conductivity results from flash sintering are in full agreement with those calculated from the percolation model. *Published by AIP Publishing.*
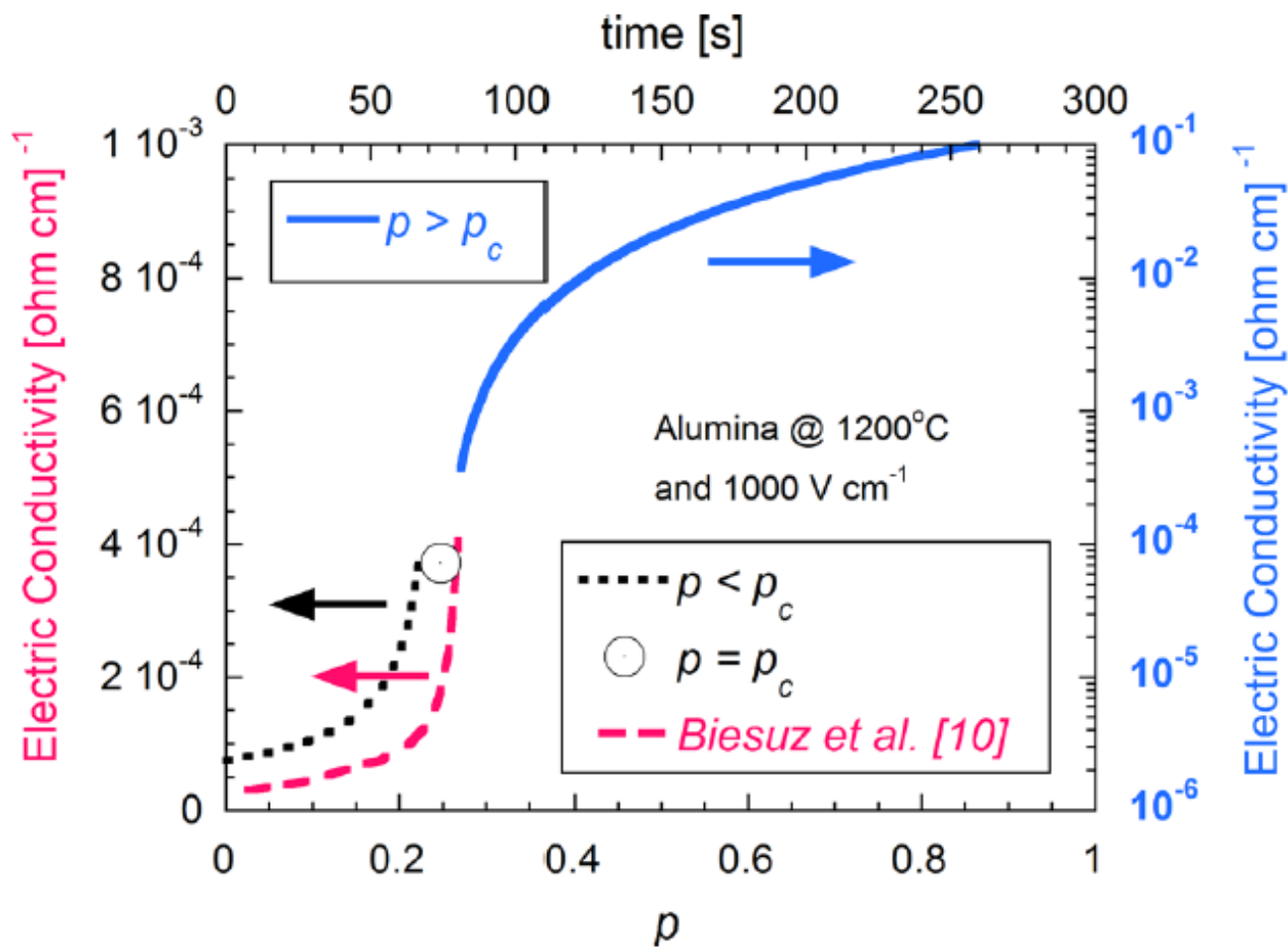[http://dx.doi.org/10.1063/1.4980853]

FIG. 1. Electric conductivity of α-Al$_2$O$_3$ nanoparticles subjected to flash sintering at 1200 °C under 1000 V·cm^{-1} versus time (top x-axis) (Ref. [10]), and the volume fraction of the melt p (bottom x-axis). The experimental (red dashed-curve) coincides with the calculated (dotted black-curve) from the percolation model. The flash "incubation time" of 81 s was adjusted to the percolation threshold at $p_c = 0.247$ (open circle).

Invasion Percolation Model via surface softening

1. *Joule heating at critical particle contacts* ➜ *local melting.*

2. *Incubation time is associated with the percolation threshold.*

3. *Current percolation through the melt.*

   No current limit: *Dielectric breakdown*

   Current limit: Current control forms local melts throughout the specimen ➜ *Particle wetting and rearrangement by capillary forces.*

On thermal runaway and local endothermic/exothermic reactions during flash sintering of ceramic nanoparticles

Rachman Chaim[1,*] and Claude Estournès[2]

[1] Department of Materials Science and Engineering, Technion – Israel Institute of Technology, 32000 Haifa, Israel

[2] Université de Toulouse, CIRIMAT, CNRS INPT UPS, Université Paul-Sabatier, 118 route de Narbonne, 31062 Toulouse Cedex 9, France
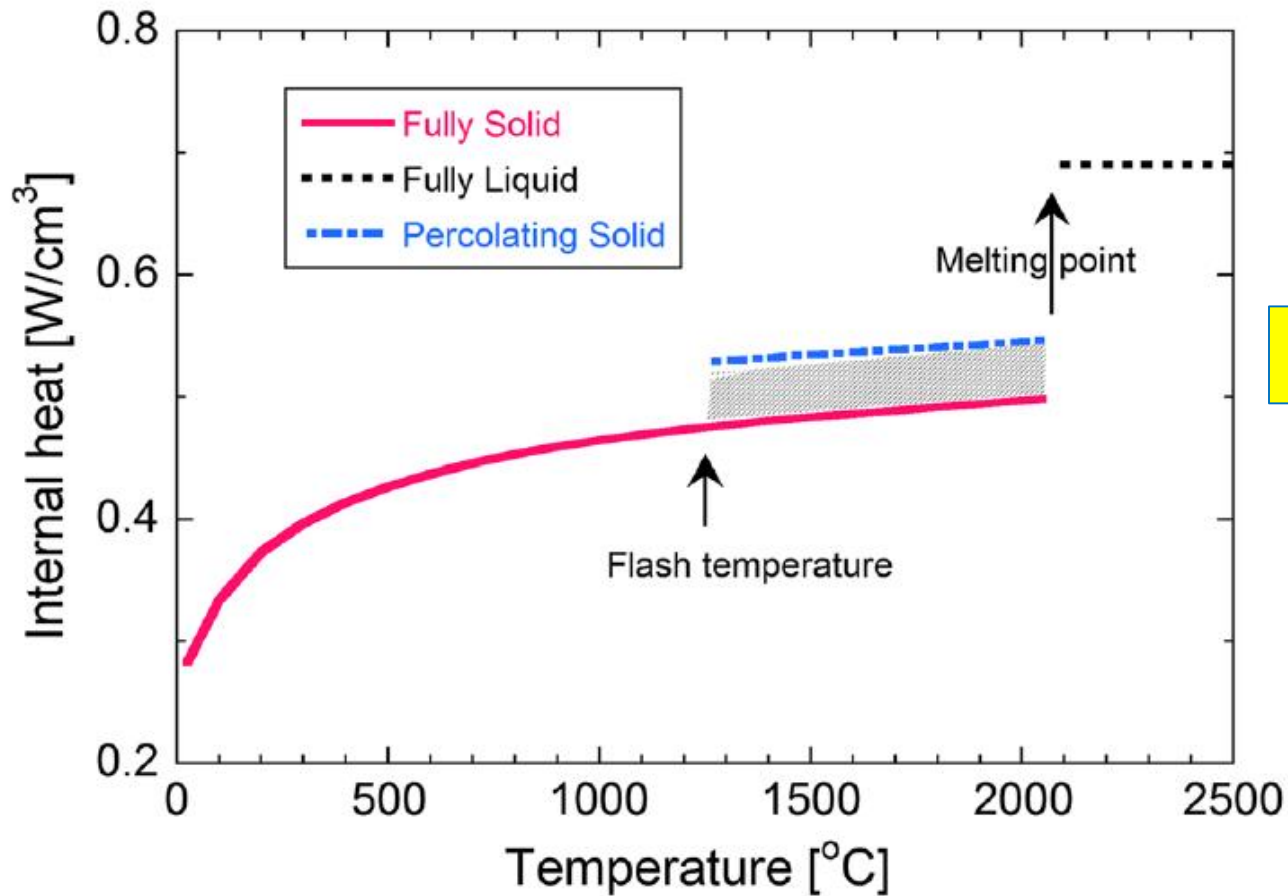
Theory

Heat transfer from nanoparticles
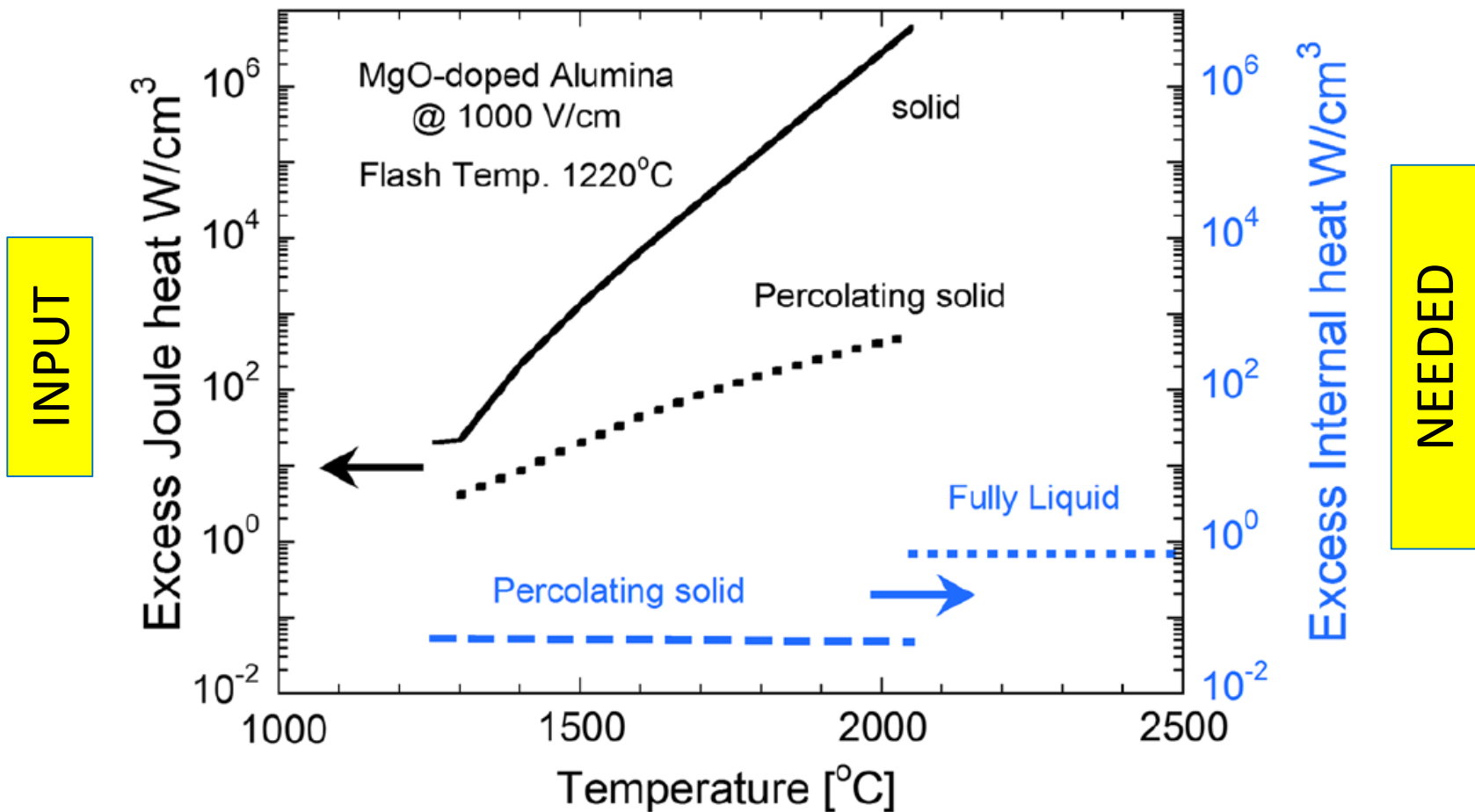
Conduction heat transfer

Radiation heat transfer

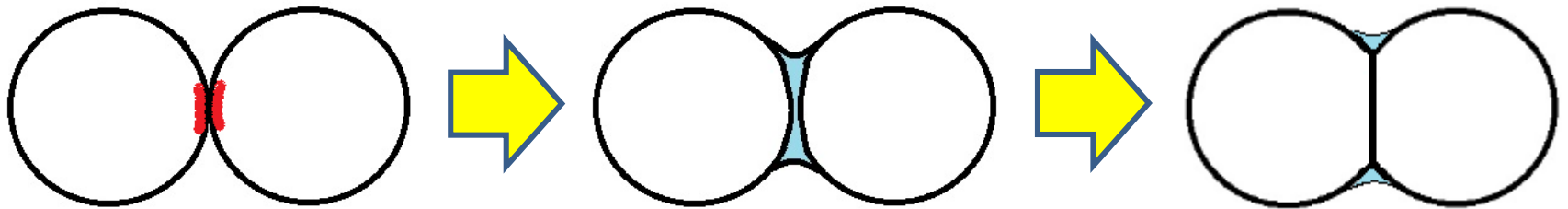**Heat balance at flash event**

Thermodynamics of Liquid-film formation

Alumina

Chaim, Estournes, J. Mater. Sci. 53 (2016) 6378-89

Thermodynamics *of Liquid-film formation*

*Chaim, Estournes, J. Mater. Sci. **53** (2016) 6378-89*

Densification during Flash Sintering
by Liquid-film Capillary

Particle diameter [nm]	50	100	200	500	1 μm
Capillary pressure [MPa]	56	28	14	5.6	2.8

Hot Press Values

Regular Article

On the kinetics of liquid-assisted densification during flash sintering of ceramic nanoparticles

Rachman Chaim

Department of Materials Science and Engineering, Technion – Israel Institute of Technology, Haifa 32000, Israel

A R T I C L E   I N F O

Liquid-film assisted Sintering

The capillary force in the presence of liquid is equivalent to externally applied pressure of:

$$P_{ext} = 2\pi\sqrt{2} \cdot \frac{\gamma_{lv}}{r_p} \cos\theta$$

γ_{lv} - *liquid-vapor surface energy*

r_p - *particle radius*

θ - *wetting angle*

R.B. Heady, J.W. Cahn, Metall Trans 1 (1970) 185-189

Liquid-film Sintering Kinetics

The main question is:

Are the kinetics of these processes fast enough to fulfill a few seconds durations of the flash sintering process.

Therefore, our main target is to evaluate the time scale of the wetting and rearrangement processes using the existing models.

Electro-osmotic / Capillary liquid flow

- *We checked the electro-osmotic forces and velocities and capillary forces and velocities.*

- *For electric fields perpendicular and parallel to the liquid at the contact.*

- *For jammed particles and free-to-move particles.*

(a)   (b)   (c)

Chaim, Scripta Mater. 158 (2019) 88-90
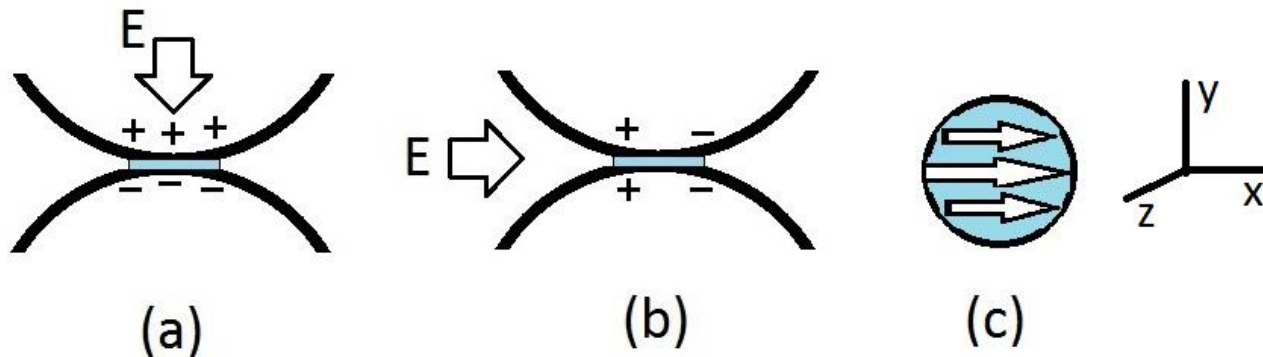
Electro-osmotic liquid flow

▪ *The terminal velocity, V of the molecule (cation with two anions)*

in the liquid film at the particle contact subjected to external

electric field parallel to the film is:

$$V = \frac{Z \cdot e\, E}{4\pi a}$$
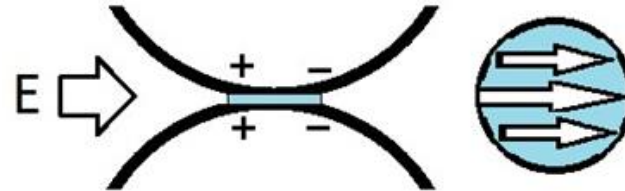
Z - cation valence electrons   *e - electron charge*

E - electric field η *- viscosity of the liquid*

a - average molecule radius

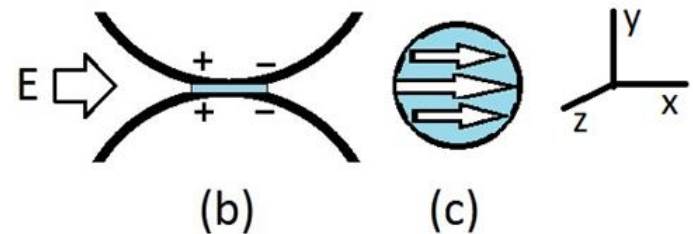*Chaim, Scripta Mater. 158 (2019) 88-90*

Electro-osmotic liquid flow

- *The flow speed of the anionic polyhedra under the electric field at the edges of the liquid film and against the drag by the positive ions at the double-layer.*

MgO-doped Al_2O_3 @ 1000 V/cm

Al_2O_3 melt: $Z = 3$, $a = 0.319$ nm

Viscosity of 0.044 [Pa·s] at 2323K

(b)   (c)

Terminal velocity: 272 $\mu m \cdot s^{-1}$

Chaim, Scripta Mater. 158 (2019) 88-90

Electro-osmotic liquid flow

- *The directional symmetry of the electric field imposes directional flow in the field direction (Posieuille flow).*

- *If one particle is free of geometrical constraints, the viscous drag may shear it from its neighbor (Couette flow).*

Particle rearrangement is accelerated by particle sliding and rotation assisted by the electro-osmotic flow.

Chaim, Scripta Mater. 158 (2019) 88-90
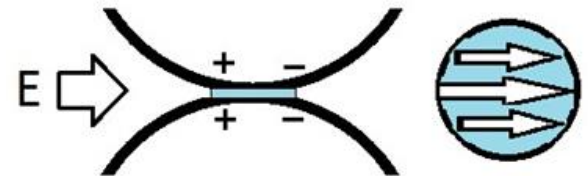
Capillary driven liquid flow

- *Superposition of the acting forces to highlight the effect of the capillary forces on the flow of the Liquid-film.*

- *The liquid at the contact leads to capillary forces that are balanced by the viscous drag.*

- *We assumed that the melt at the contact flows radially between the two particles.*

Capillary driven liquid flow

- *Following the velocity profile between two fixed and parallel disc surfaces (Posieuille flow).*

- *The maximum radial flow rate of the liquid due to pressure gradient ΔP expressed as:*

$$u_{max} = \frac{\Delta P \, (\delta_b)^2}{2 \, r \, ln\left(\frac{r_2}{r_1}\right)}$$

δ_b is the liquid film thickness,
η is the liquid viscosity

r is the radial distance somewhere between r_1 (disc center) and r_2 (disc perimeter) where the *external* pressure gradient exist

The case of particle neck wetting

- *The driving force for wetting is the internal capillary force due to the curvatures at the liquid meniscus.*

- *The pressure gradient is:*

$$\Delta P = \gamma_{lv} \left(\frac{1}{r_2} - \frac{2}{\delta_b} \right)$$

γ_{lv} is the liquid-vapor surface energy
r_2 is the contact radius

Two curvatures with positive and negative signs

The Maximum flow velocity

- *The maximum flow velocity at the film perimeter, r_2, is:*

$$u_{max} = \gamma_{lv} \left(\frac{1}{r_2} - \frac{2}{\delta} \right) \frac{(\delta_b)^2}{2 \, r_2 \, ln\left(\frac{r_2}{r_1}\right)}$$

The above equations based on the steady state flow conditions. Nevertheless, we are interested in the liquid flow at the early stages of the wetting hence, our calculations may be estimates.

The Maximum flow velocity

- *Example:* MgO-doped Al_2O_3

- r_p = 50 nm, γ_{lv} = 0.7 J·m^{-2}

- Liquid film thickness of δ_b = 1.5 nm

- Assuming a dry neck to particle radius ratio 0.02 in the green compact, hence $r_1 = 0.02 \cdot r_p$

Wetted neck to particle radius ratio of 0.10 and 0.20 that correspond to neck radii of 5 nm and 10 nm

Maximum flow velocities of 1.04 m·s^{-1} and 0.48 m·s^{-1}

The Maximum flow velocity

- *These extremely high velocities indicate that liquid flow is instantaneous (i.e. from the time of its formation at the neck center) hence the neck is fully wet and the liquid reaches the neck meniscus within tens of nanoseconds.*

- *Comparison of the ion velocities in the melt:*

Capillary force effect >> Electric field effect

Is there any residual amorphous phase?

- *Solidification of the melt by epitaxial (heterogeneous) nucleation*

- *Most favorable on its counterpart solid substrate.*

- *The nucleation energy barrier needed for such a critical nucleus:*

$$\Delta G^*_{het} = \frac{16\,\pi}{3}\frac{(\gamma_{sl})^3}{(\Delta G_v)^2}S(\theta)$$

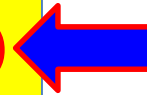γ_{sl} - *solid-liquid specific interface energy*

ΔG_v - *free energy change per unit volume due to the nucleus*

$S(\theta)$ - *nucleus shape factor that depends on the contact angle θ*

Is there any residual amorphous phase?

- *Solidification of the melt by epitaxial (heterogeneous) nucleation*

- *Most favorable on its counterpart solid substrate.*

- *The nucleation energy barrier needed for such a critical nucleus:*

$$\Delta G_{het}^* = \frac{16\,\pi}{3}\frac{(\gamma_{sl})^3}{(\Delta G_v)^2}\,S(\theta)$$

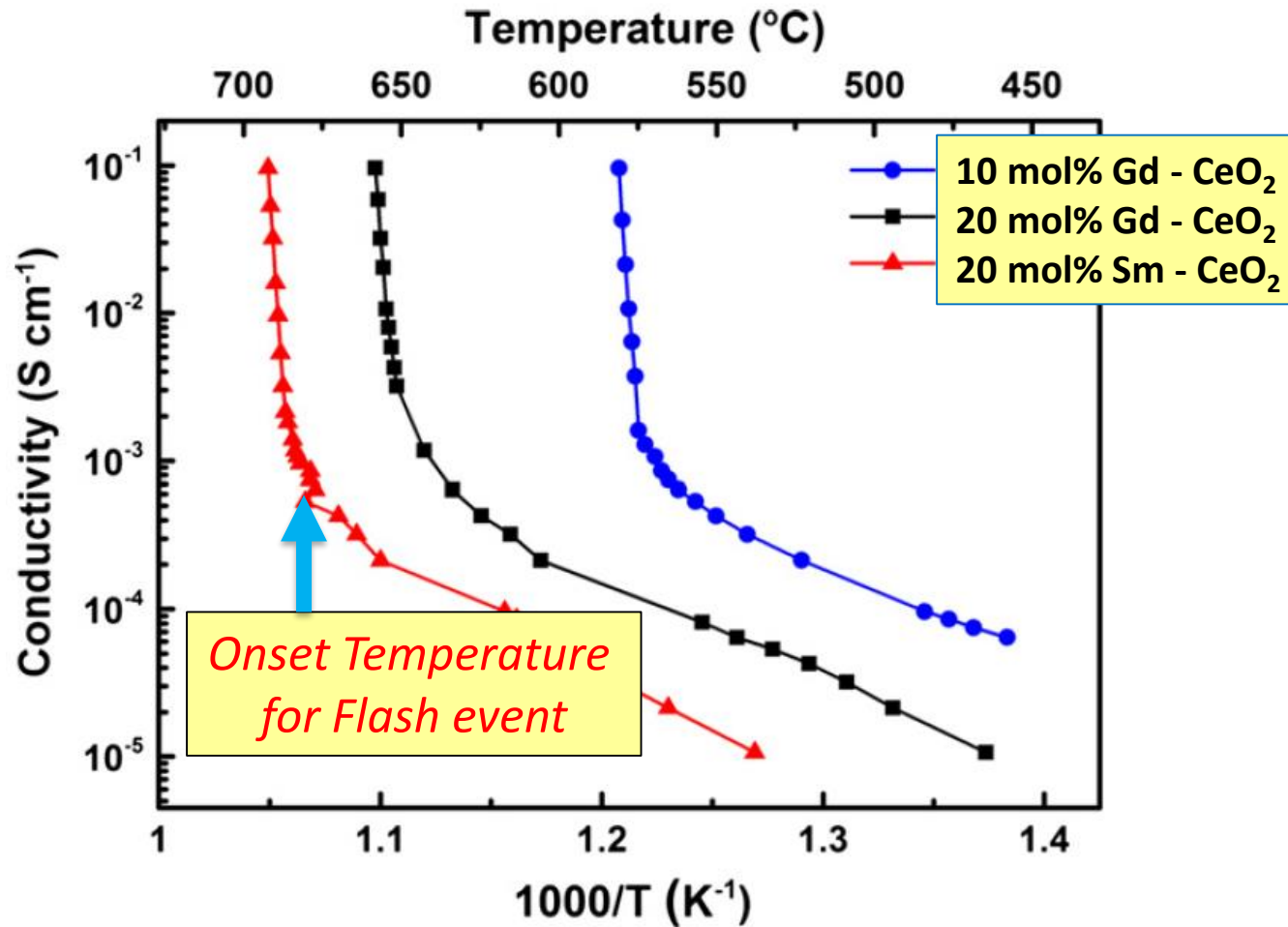γ_{sl} *- solid-liquid specific interface energy*

ΔG_v *- free energy change per unit volume due to the nucleus*

$S(\theta)$ *- nucleus shape factor that depends on the contact angle* θ

Sudden & drastic increase in *dissipated Power*

R. Raj *J. Am. Ceram. Soc.* **99** (2016) 1400
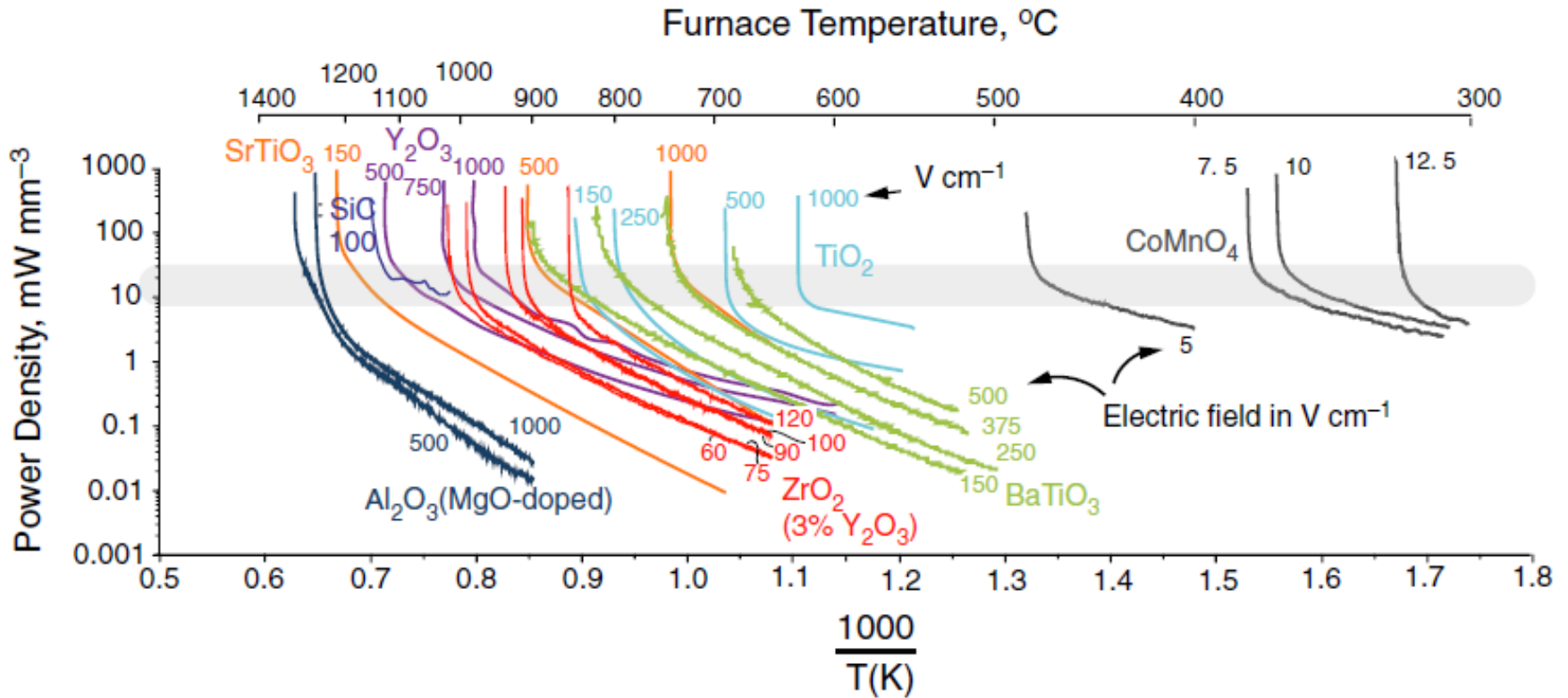
Conductivity increase vs. *furnace* temperature

*T. Jiang et al. J. Am. Ceram. Soc. **98** (2015) 1717*

Numerical model for particle size effects on flash sintering temperature of ionic nanoparticles

Rachman Chaim[1,*] (iD)

[1] Department of Materials Science and Engineering, Technion – Israel Institute of Technology, 32000 Haifa, Israel
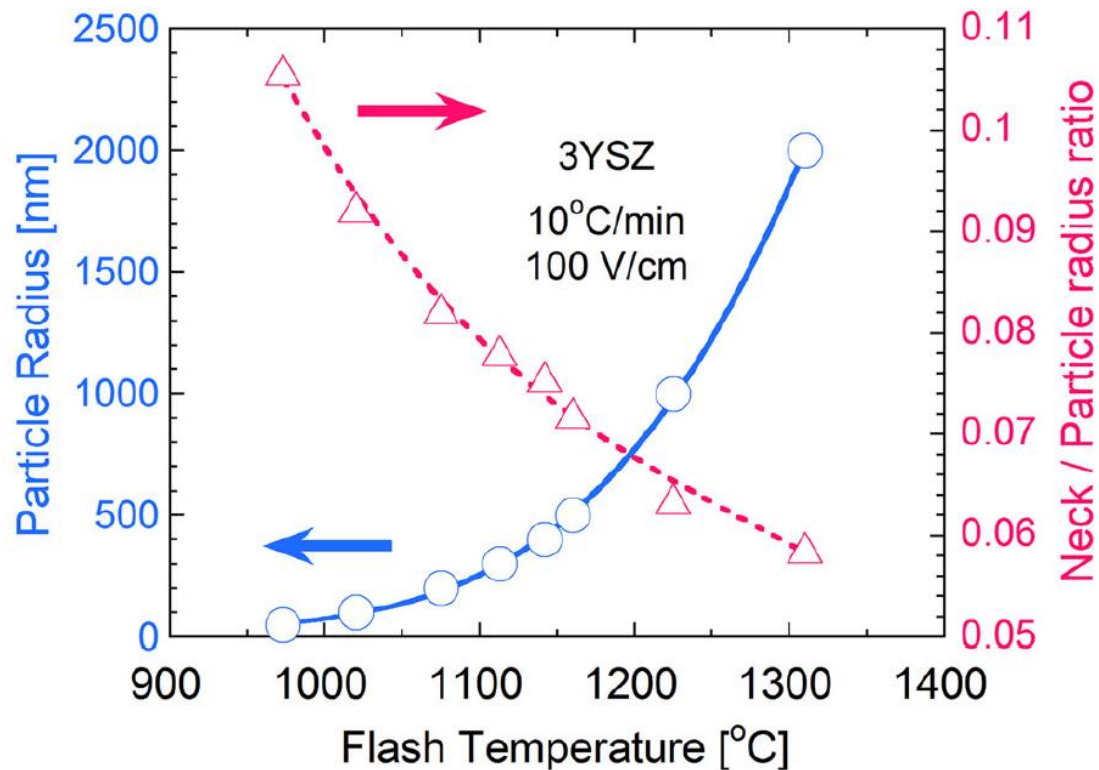
Figure 6 Calculated flash temperature versus particle radius and neck to particle radius ratio in 3YSZ in the particle size range of 50–2000 nm.

Effects of the fundamental oxide properties on the electric field-flash temperature during flash sintering

Rachman Chaim [a,*], Claude Estournès [b]

[a] Department of Materials Science and Engineering, Technion — Israel Institute of Technology, Haifa 32000, Israel
[b] Université de Toulouse, CIRIMAT, CNRS INPT UPS, Université Paul-Sabatier, 118 route de Narbonne, F-31062 Toulouse cedex 9, France
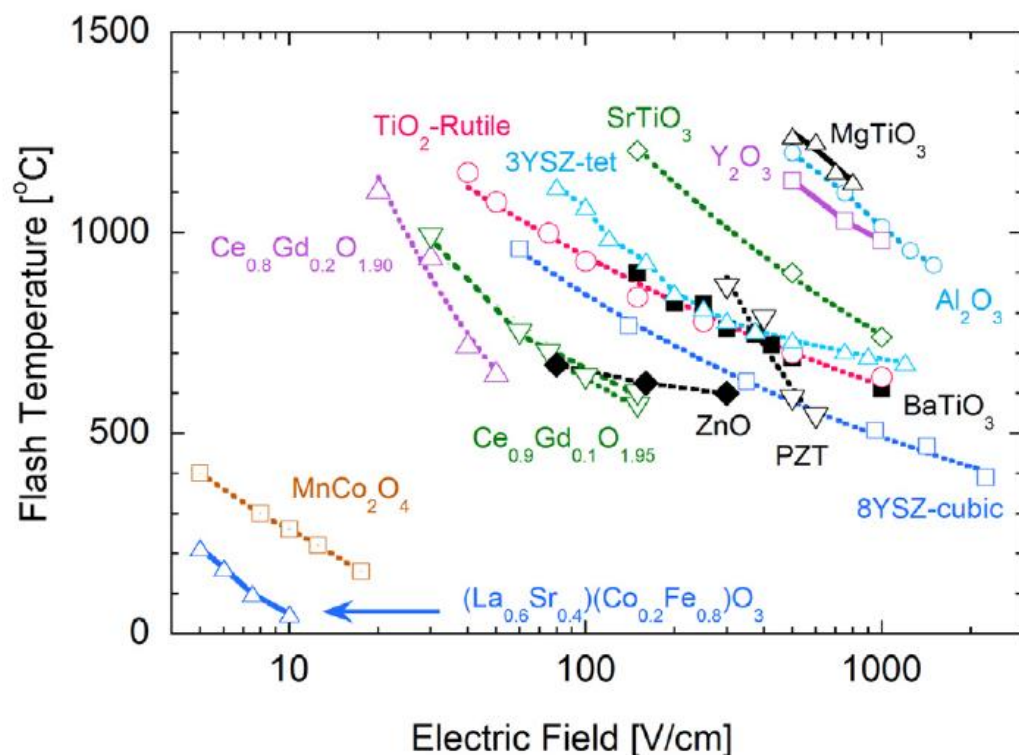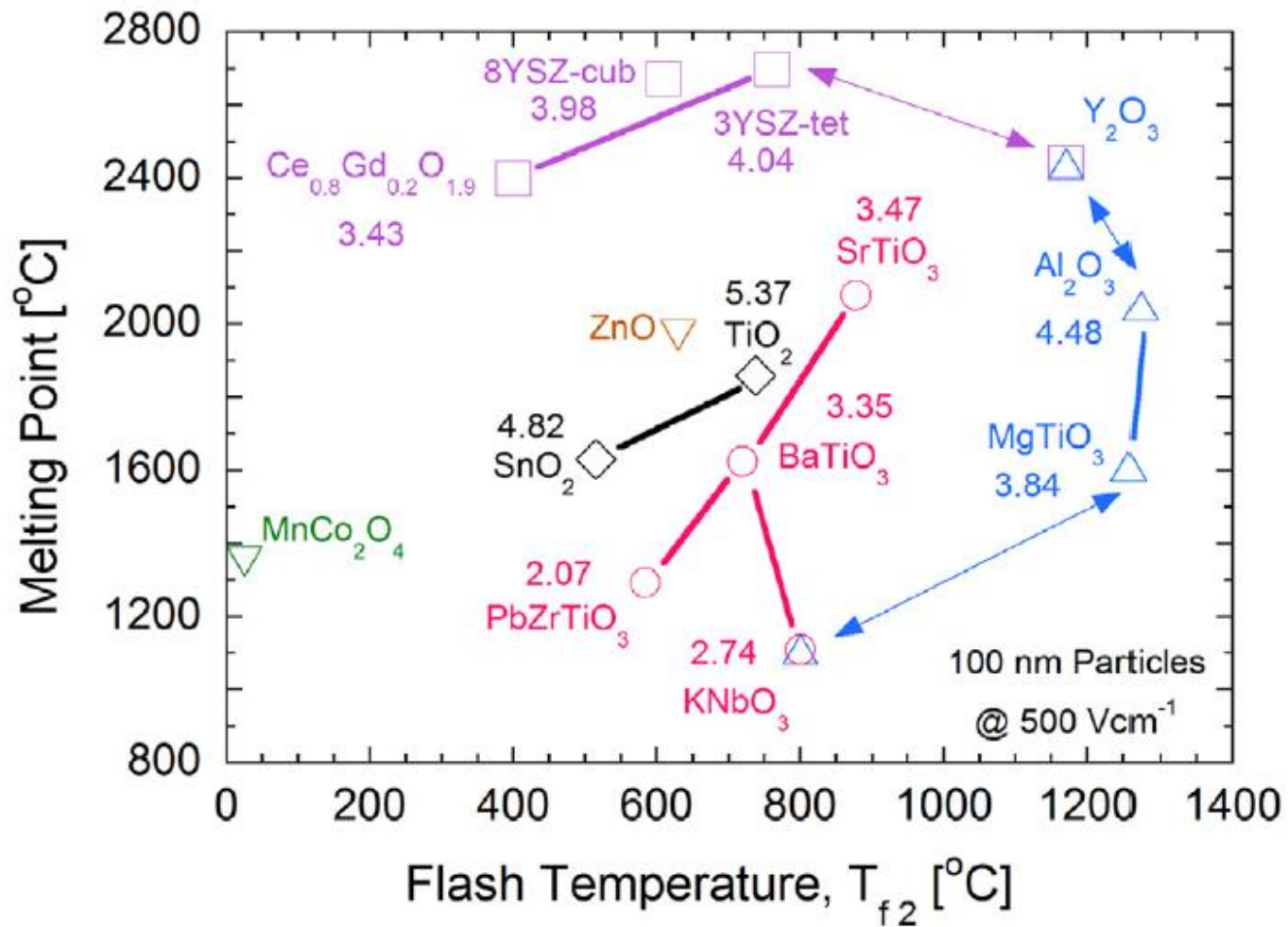

Fig. 1. Experimental flash temperature–electric field relations in different oxides: Al_2O_3 [1], $BaTiO_3$ [10], $Ce_{0.9}Gd_{0.1}O_{1.95}$ [11,12], $Ce_{0.8}Gd_{0.2}O_{1.90}$ [13], $(La_{0.6}Sr_{0.4})(Co_{0.2}Fe_{0.8})O_3$ [12], $MgTiO_3$ [16], $MnCo_2O_4$ [17], $Pb(Zr_{0.52}Ti_{0.48})O_3 - PZT$ [18], $SrTiO_3$ [20], TiO_2 [21], Y_2O_3 [22], 3YSZ [23], 8YSZ [24], and ZnO [25].
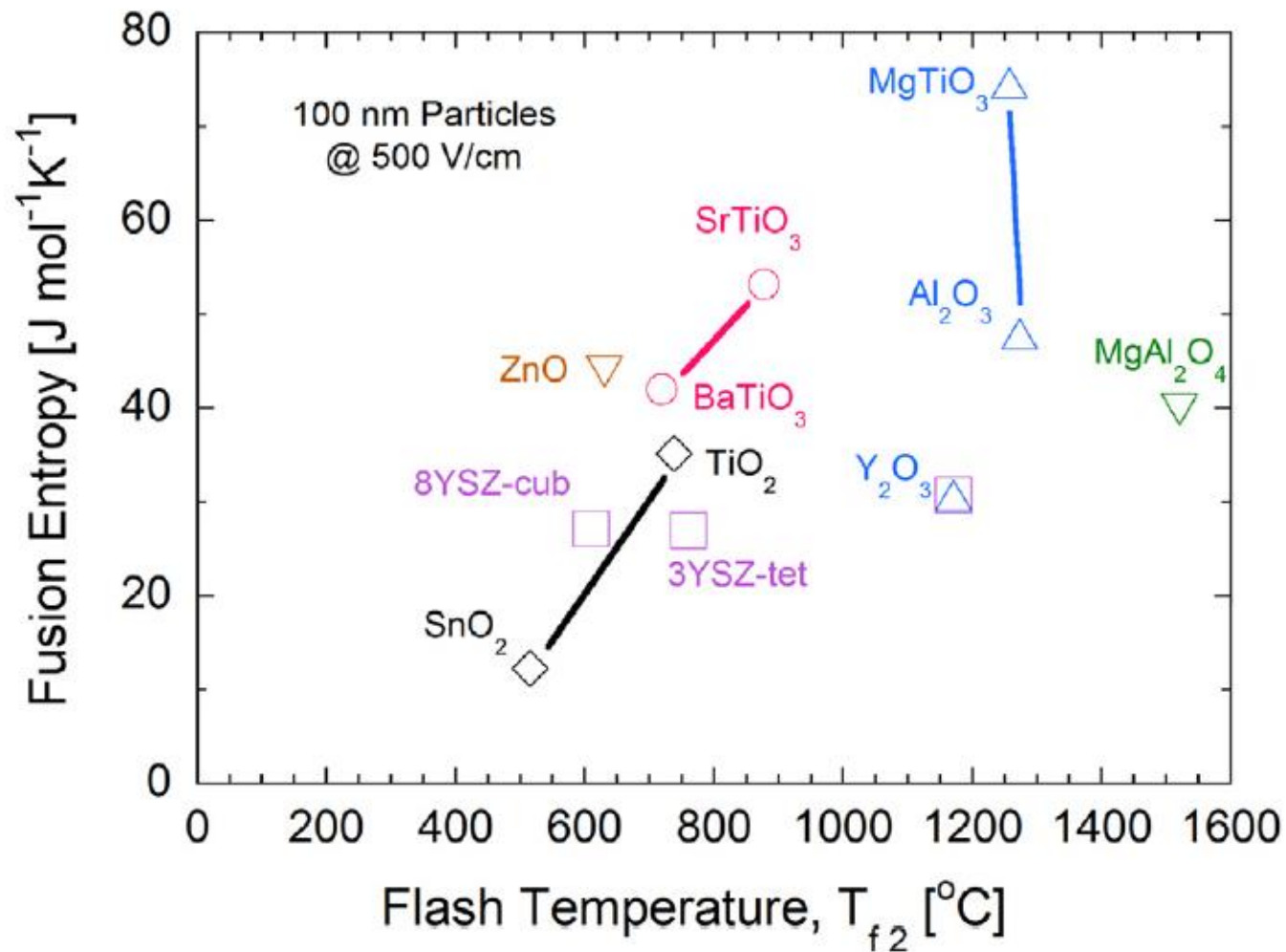
the 'structure-field maps' of Goldschmidt

*Chaim, Estournes, Scripta Mater **163** (2019) 130-132*

Fig. 3. Fusion entropy–flash temperature diagram of oxides normalized for the 100 nm particle size under the 500 V·cm^{-1} electric field. The lines used as guidelines only to highlight the oxides with similar crystal structure.

*Chaim, Estournes, Scripta Mater **163** (2019) 130-132*

Summary & Conclusions

- *The kinetics of flash sintering assisted by a liquid-film is in agreement with the experimental time scales of a few seconds.*

- *Joule heat provides the activation energy for local surface softening / melting.*

- *Thermal runaway is an endothermic local melting of the particle contacts. The transient liquid solidifies after the particle rearrangement.*

Summary & Conclusions

- *Homologous crystallization of the local melt after particle rearrangement is energetically preferred due to the exothermic nature of solidification.*

Thank you for your attention